CHINESE OPTICS LETTERS

Vol. 21, No. 10 | October 2023

Generation of shaping nondiffracting structured caustic beams on the basis of stationary phase principle

Rijian Chen (陈日坚), Yile Shi (施逸乐), Ning Gong (弓 宁), Yefeng Liu (刘叶枫), and Zhijun Ren (任志君)*

Key Laboratory of Optical Information Detecting and Display Technology, Zhejiang Normal University, Jinhua 321004, China

*Corresponding author: renzhijun@zjnu.cn

Received March 24, 2023 | Accepted May 11, 2023 | Posted Online August 31, 2023

On the basis of the stationary phase principle, we construct a family of shaping nondiffracting structured caustic beams with the desired morphology. First, the analytical formula of a nondiffracting astroid caustic is derived theoretically using the stationary phase method. Then, several types of typical desired caustics with different shapes are numerically simulated using the obtained formulas. Hence, the key optical structure and propagation characteristics of nondiffracting caustic beams are investigated. Finally, a designed phase plate and an axicon are used to generate the target light field. The experimental results confirm the theoretical prediction. Compared with the classical method, the introduced method for generating nondiffracting caustic beams is high in light-energy utilization; hence, it is expected to be applied conveniently to scientific experiments.

Keywords: nondiffracting structured caustic beams; phase plate; stationary phase method; axicon.

DOI: 10.3788/COL202321.102601

1. Introduction

In contrast with classical optics theory, catastrophe optics theory is primarily introduced to describe and reveal other unorthodox optical phenomena that are changed abruptly by optical intensity. It is called a "catastrophe" because optical bifurcation and singularity are typically accompanied by a dramatic change in optics. The theory of catastrophe optics is an important complement to classical optics theory[1]. Catastrophes naturally occur in generic topologies in a wide range of systems[2,3]. Optical caustics are concrete manifestations of catastrophe theory. When light is focused such that rays intersect and coalesce by refracting or reflecting in rough and uneven media, it forms focal lines or surfaces called caustics, which are an envelope of light rays that are typically accompanied by an abrupt increase in concentrated intensity. Some catastrophe optics morphologies of caustics and their diffraction patterns have been theoretically researched by some researchers[4–6].

In daily life, optical caustics are naturally focused because their wavefronts are perturbed by random inhomogeneities. For example, people can see natural optical caustics, such as sunlight refracted or reflected on a wavy water surface, which occur as bright lines of high intensity on the floor of shallow water and the bottom of a bridge[7,8]. Apparently, natural caustic light is flickering and its caustics structure is unstable. Hence, constructing stable caustics beyond those that occur naturally is particularly important for some research fields. In the pioneering work of Thom[1], Whitney[9], and Arnold[10], stable caustics in physics exhibit an isomorphic relationship with the elementary topological structures of catastrophe theory. In accordance with Thom's catastrophe theory, structurally stable caustics can be classified into seven standard forms: folds, cusps, swallowtails, butterflies, and elliptical, hyperbolic, and parabolic umbilicus mutations[6,11,12]. Notably, some famous structured lights can be understood in terms of caustics. For example, the well-known Airy[13,14] and Pearcey[15] beams are simply standard classification caustics, i.e., "fold" and "cusp" catastrophes[4,5]. Subsequently, the optical caustics concept is also used to customize and shape other structured beams, such as self-accelerating beams[16–18], self-accelerating surface plasmon beams[19–22], Mathieu beams[23,24], and other caustic beams[25–27]. Constructing caustic beams with a stable structure has become a popular research topic because of the novel spatial light-field distribution, unique optical properties, and practical application values of such beams[28,29].

Different scientific experiments require various shaping nondiffracting structured beams. The limited number of caustic beams available at present restricts their applications. Apparently, the design of new caustic beams with a prescribed caustics is an important and challenging task. On the basis of the inherent connection between optical wavefront and natural caustics focusing, some researchers have constructed complex structured beams by applying catastrophe theory. However, such structured beams are not propagation-invariant beams, i.e., they are not nondiffracting beams[7,13,30]. In 2020,

Zannotti *et al.* generated several types of nondiffracting caustic beams with a customizable intensity profile[31]. In their work, the nature of the method they used to generate caustic beams was Fourier transform. Hence, they must produce a transverse Fourier spectrum of the wavefield limited to the ring. In the work of Zannotti, the utilization rate of light energy was particularly low during the generation of nondiffracting caustic beams. In this study, in order to avoid using circular slits to generate caustic beams, since it greatly limits the utilization of light energy[31], we introduce a stationary phase method for generating nondiffracting beams along the desired caustic. Consequently, a series of caustic beams is generated using a phase plate and an axicon. Compared with that in Ref. [31], the introduced method for generating caustic beams considerably improves the utilization rate of light energy.

2. Theory

Understanding the caustics concept requires the aid of physical optics and the simpler ray model of geometrical optics. Catastrophe optics can link geometrical optics with wave optics. Geometrical optics can readily define the topology of a caustic through the envelope of a family of rays, while wave optics can reveal the diffraction pattern and correctly quantify its intensity[5]. Apparently, the intensity maxima follow the shapes of the caustic lines, which are the singularities of gradient maps from the optical wavefront. Notably, the wavefronts described here are the curved reflecting surfaces perpendicular to the optical rays of geometrical optics. Hence, the optical wavefront is also called the "geometrical optics wavefront"[5]. The relation between caustic shape and geometrical optics wavefront is given by the following expression[31]:

$$\mathbf{r}_c(\varphi) = \frac{1}{k_\perp}[\Phi''(\varphi)\boldsymbol{\mu}(\varphi) - \Phi'(\varphi)\boldsymbol{\mu}'(\varphi)], \tag{1}$$

where $\mathbf{r}_c(\varphi) = (x, y)$ is a parameterized caustic shape, $\boldsymbol{\mu}(\varphi) = (\cos\varphi, \sin\varphi)$ is a unit vector, and $k_\perp$ is a transverse wavenumber. To generate the desired caustic with a given parameterized $\mathbf{r}_c(\varphi)$, the geometrical wavefront shaping (i.e., physical phase function) Φ must be calculated by solving Eq. (1). When the phenomenon of caustics is described, the concepts of geometrical and wave optics must work together.

As typical caustic beams, we first derive the phase function of an astroid caustic. The expression of the astroid curve[7] can be written as

$$\mathbf{r}_c(\varphi) = \frac{1}{k_\perp}\begin{bmatrix}(3q - 2q\sin^2\varphi)\sin\varphi \\ (3q - 2q\cos^2\varphi)\cos\varphi\end{bmatrix}. \tag{2}$$

By substituting Eq. (2) into Eq. (1) and then solving the differential equation for the parameterized astroid curve, the following equation can be obtained:

$$\Phi(\varphi) = -\frac{q}{2}\sin(2\varphi), \tag{3}$$

where q is an integral number that determines the geometrical wavefront or physical phase function of an astroid caustic. In an experiment, the corresponding physical phase of the geometrical wavefront can be produced.

In our scheme, the obtained wavefront shaping Φ is used to generate nondiffracting structured caustic beams on the basis of the stationary phase principle. The propagation of a modulated beam in free space can be described by Fresnel diffraction. The Fresnel diffraction integral in cylindrical coordinates is

$$U(\rho,\theta,z) = \frac{-i}{\lambda z}\exp(ikz)\int_0^\infty\int_0^{2\pi} U_0(r,\varphi)\exp\left[\frac{ik}{2z}(r^2+\rho^2)\right] \times \exp\left[-\frac{ik}{z}\rho r\cos(\varphi-\theta)\right] r\mathrm{d}r\mathrm{d}\varphi, \tag{4}$$

where λ is the wavelength of the light beam, $k = 2\pi/\lambda$ is the wavenumber, $U(\rho,\theta,z)$ represents the complex amplitude distribution of the light field in free space, ρ and θ are the radial distance and azimuth angle of the beam in free space, respectively, z is the axial propagation distance, and $U_0(r,\varphi)$ is the complex amplitude distribution of the initial light field ($z = 0$) modulated by phase elements. In our scheme, an axicon phase is necessary to generate nondiffracting structured caustic beams on the basis of the stationary phase principle. The collimated parallel light is successively incident to a phase plate and the axicon. Hence, the initial optical field can be written as

$$U_0(r,\varphi) = A(\varphi)T(r), \tag{5}$$

where $A(\varphi) = \exp[i\Phi(\varphi)]$ is the transmission function of the phase plate, and $T(r)$ is the complex amplitude transform function of the axicon[32]. The radial phase distribution of the axicon is

$$T(r) = \begin{cases}\exp[-ik(n_0-1)\theta_0 r], & r \le R, \\ 0, & r \ge R,\end{cases} \tag{6}$$

where n_0 is the refractive index of the axicon, θ_0 is the base angle of the axicon, which is typically a small angle, and R is the aperture radius of the entrance pupil.

By substituting Eq. (6) and $A(\varphi) = \exp[i\Phi(\varphi)]$ into Eq. (5) and then substituting the resulting expression into Eq. (4), the following equation can be obtained:

$$U(\rho,\theta,z) = \frac{-i}{\lambda z}\exp(ikz)\exp\left(\frac{ik}{2z}\rho^2\right) \times \int_0^R r\mathrm{d}r\exp[-ik(n_0-1)\theta_0 r]\exp\left(\frac{ik}{2z}r^2\right) \times \int_0^{2\pi}\mathrm{d}\varphi\exp[i\Phi(\varphi)]\exp\left[-\frac{ik}{z}\rho r\cos(\varphi-\theta)\right]. \tag{7}$$

In deriving Eq. (7), the following Jacobi–Anger expansion should be used[33]:

$$\exp(iz\ \cos\ \theta) = \sum_{m=-\infty}^{\infty} (i)^m J_m(z) \exp(im\theta), \tag{8}$$

where J_m is the mth-order Bessel function of the first kind. On the basis of Eq. (8), the following expression can be obtained:

$$\exp\left[-\frac{ik}{z}\rho r\ \cos(\varphi-\theta)\right] = \sum_{m=-\infty}^{\infty} (-i)^m J_m\left(\frac{k}{z}\rho r\right) \times \exp[-im(\varphi-\theta)]. \tag{9}$$

By substituting Eq. (9) into Eq. (7), the following equation can be obtained:

$$\begin{aligned} &U(\rho,\theta,z) \\ &= \frac{-i}{\lambda z}\ \exp(ikz)\exp\left(\frac{ik}{2z}\rho^2\right) \\ &\times \sum_{m=-\infty}^{\infty} (-i)^m \exp(im\theta) \int_0^{2\pi} \mathrm{d}\varphi\ \exp\{i[\Phi(\varphi)-m\varphi]\} \\ &\times \int_0^R r\mathrm{d}r J_m\left(\frac{k}{z}\rho r\right) \exp\left\{ik\left[\frac{r^2}{2z}-(n_0-1)\theta_0 r\right]\right\}. \end{aligned} \tag{10}$$

Because Eq. (10) is double integrals, its analytic result is difficult to obtain directly. The stationary phase principle is a method for simplifying the oscillatory integral that is difficult to solve directly with the form $\int g(r)\exp[ikf(r)]\mathrm{d}r$ when $k\to\infty$[34]. For Eq. (10), we set $f(r)=[r^2/(2z)-(n_0-1)\theta_0 r]$ and $g(r)=J_m(k\rho r/z)r$. On the basis of $f'(r)|_{r=r_0}=r_0/z-(n_0-1)\theta_0=0$, the stationary phase point can be obtained when $r_0=(n_0-1)\theta_0 z$. When $r=r_0\in(0,R)$, the maximum nondiffracting distance $z_{\max}=R/[(n_0-1)\theta_0]$ is obtained. The distribution of the optical field at $0<z<z_{\max}$ is

$$\begin{aligned} U(\rho,\theta,z) \approx &\frac{-ik_r\sqrt{\lambda z}}{\lambda k}\ \exp(ikz)\exp\left(\frac{ik}{2z}\rho^2\right) \\ &\times \exp\left\{i\left[\frac{-k(n_0-1)^2\theta_0^2 z}{2}+\frac{\pi}{4}\right]\right\} \\ &\times \sum_{m=-\infty}^{\infty} (-i)^m J_m(k_r\rho)\exp(im\theta) \\ &\times \int_0^{2\pi} \mathrm{d}\varphi\ \exp\{i[\Phi(\varphi)-m\varphi]\}, \end{aligned} \tag{11}$$

where $k_r=k(n_0-1)\theta_0$. Equation (11) shows that various caustic shapes can be achieved by substituting the corresponding phase function Φ. By substituting Eq. (3) into Eq. (11), the following equation can be obtained:

$$\begin{aligned} U(\rho,\theta,z) = &\frac{-ik_r\sqrt{\lambda z}}{\lambda k}\ \exp(ikz)\exp\left(\frac{ik}{2z}\rho^2\right) \\ &\times \exp\left\{i\left[\frac{-k(n_0-1)^2\theta_0^2 z}{2}+\frac{\pi}{4}\right]\right\} \\ &\times \sum_{m=-\infty}^{\infty} (-i)^m J_m(k_r\rho)\exp(im\theta) \\ &\times \int_0^{2\pi} \mathrm{d}\varphi\ \exp\left\{i\left[-\frac{q}{2}\ \sin(2\varphi)-m\varphi\right]\right\}. \end{aligned} \tag{12}$$

To solve Eq. (12), the following expression should be used[35]:

$$\int_0^{\pi} \mathrm{d}\varphi\ \exp[2im\varphi+ib\ \sin(2\varphi)] = \pi(-1)^m J_m(b). \tag{13}$$

Hence, the integral part of Eq. (12) can be written as

$$\begin{aligned} &\int_0^{2\pi} \mathrm{d}\varphi\ \exp\left\{i\left[-\frac{q}{2}\ \sin(2\varphi)-m\varphi\right]\right\} \\ &= \pi[1+\exp(-im\pi)]\times(-1)^{\frac{-m}{2}} J_{\frac{-m}{2}}\left(-\frac{q}{2}\right). \end{aligned} \tag{14}$$

We make the substitution $m=2n$ (n is an integer) in the following derivation process. By substituting Eq. (14) into Eq. (12), we obtain the complex amplitude expression of the astroid caustic,

$$\begin{aligned} U(\rho,\theta,z) = &\frac{-ik_r\sqrt{\lambda z}}{2}\exp(ikz)\exp\left(\frac{ik}{2z}\rho^2\right) \\ &\times \exp\left\{i\left[\frac{-k(n_0-1)^2\theta_0^2 z}{2}+\frac{\pi}{4}\right]\right\} \\ &\times \sum_{n=-\infty}^{\infty} J_{2n}(k_r\rho)\exp(2in\theta) \\ &\times \left[1+\exp(-2in\pi)\right] J_{-n}\left(-\frac{q}{2}\right). \end{aligned} \tag{15}$$

The intensity distribution of the astroid caustic is

$$I(\rho,\theta,z) = U(\rho,\theta,z)U^*(\rho,\theta,z), \tag{16}$$

where * denotes a complex conjugate. From the sum expression given in Eq. (15), one readily knows that the radial wavenumber of each order Bessel function is independent of the propagating distance z. In addition, all Bessel functions have the same transverse wavenumbers. Apparently, a superposition of nondiffracting beams with the same transverse wavenumbers still is the nondiffracting beam[36]. Equation (15) guarantees that this caustic structure is invariant in z, i.e., it is a nondiffracting structured caustic beam. To our knowledge, we obtained the analytical expression of an astroid caustic for the first time.

In general, we set $q=10$ for $\Phi(\varphi)=-q/2\ \sin(2\varphi)$, and then simulate the intensity distribution of the astroid caustic. The parameterized curve is shown in Fig. 1(a1). Figure 1(a2) is the

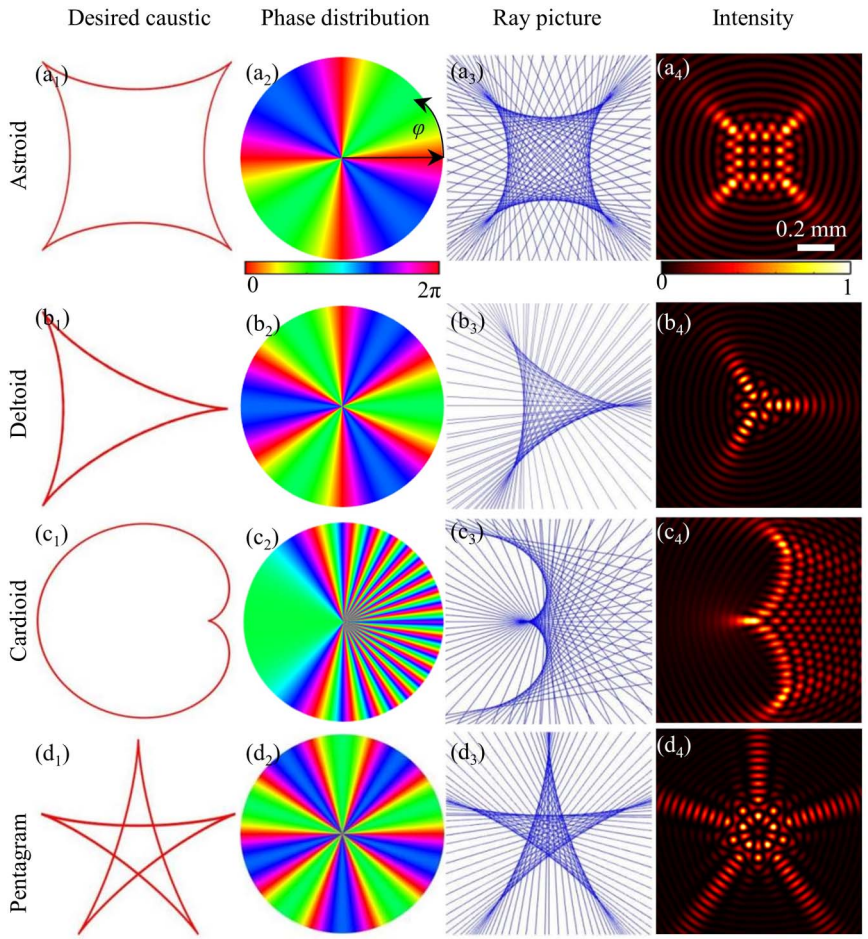

Fig. 1. Shaping nondiffracting structured caustic beams. (a) Astroid; (b) deltoid; (c) cardioid; (d) pentagram caustics. (a1)–(d1) Caustic lines; (a2)–(d2) phase distributions; (a3)–(d3) ray pictures; (a4)–(d4) simulated transverse intensities of the astroid, deltoid, cardioid, and pentagram caustics, respectively.

simulated phase map, which is mapped mod 2π. The phase function determines the properties of the astroid caustic. Using the framework of geometrical optics, the caustic lines of the beams are depicted in Fig. 1(a3). These optical rays intersect and coalesce; hence, they form focal lines or surfaces, called caustics, which are the envelope of rays. On the basis of Eq. (16), the numerical transverse intensity is simulated, as shown in Fig. 1(a4). The optical structure, shown in Fig. 1(a4), is defined by the rays and caustics and shapes the diffraction patterns of the phase map shown in Fig. 1(a2). Comparing Fig. 1(a4) and Fig. 2 in Ref. [31], the transverse maps of the two astroid caustics are the same. The diffraction pattern of the astroid caustic is concentrated around the desired caustic. Such results confirm that the stationary phase principle can be used to generate shaping nondiffracting structured caustic beams. Figure 1(a4) illustrates that the diffraction pattern of caustic beams exhibits the structure of high-intensity borders and four cusp points. Different caustics can be accompanied by varying characteristic diffraction patterns. Figures 1(b)–1(d) present the corresponding transverse light patterns for deltoid, cardioid, and pentagram caustics, respectively. The beam's intensity maxima are localized within the cusp-shaped regions of these caustics. Their corresponding curve parametric expressions are provided in Table 1. Figure 1 shows that the concepts of geometrical and

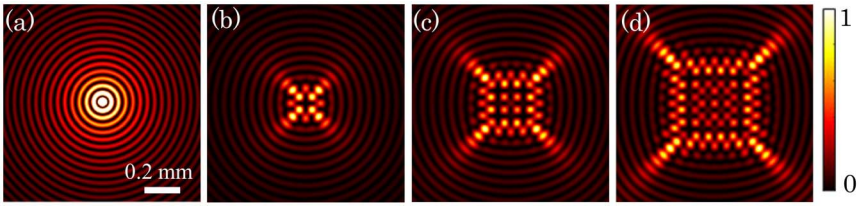

Fig. 2. Theoretical simulations of astroid caustic with different q. (a) $q = 0$; (b) $q = 5$; (c) $q = 10$; (d) $q = 15$.

Table 1. Parametric Expressions for Different Curves.

Type of Curve	$x(\varphi)$	$y(\varphi)$
Deltoid	$1/k_\perp\ [-9q\cos(3\varphi)\cos(\varphi)-3q\sin(3\varphi)\sin(\varphi)]$	$1/k_\perp\ [-9q\cos(3\varphi)\sin(\varphi)+3q\sin(3\varphi)\cos(\varphi)]$
Cardioid	$1/k_\perp\ [2q\cos(\varphi)-q\cos(2\varphi)]$	$1/k_\perp\ [2q\sin(\varphi)-q\sin(2\varphi)]$
Pentagram	$1/k_\perp\ [-25\ q\sin(5\varphi)\cos(\varphi)+5q\cos(5\varphi)\sin(\varphi)]$	$1/k_\perp\ [-25q\sin(5\varphi)\sin(\varphi)-5\ q\cos(5\varphi)\cos(\varphi)]$

wave optics work excellently when they are used to describe the phenomenon of caustics. Our scheme can be potentially extended to design other caustics-related beams[37].

On the basis of Eq. (15), we typically simulate the intensity of several types of astroid caustic with different q, as shown in Fig. 2. Figure 2 shows that the size of the astroid caustic increases with increasing the value of q. For the case of $q = 0$, the astroid caustic is degenerated into classical zero-order Bessel beams[38]. Hence, the zero-order Bessel beams can also be regarded as the special case of astroid caustic for $q = 0$. In the substitution of the phase function $\Phi(\varphi) = l\varphi$ (l is an integral) into Eq. (11), the classical Bessel beams with a spiral wavefront and carrying orbital angular momentum can be generated. The parameterized Bessel caustic, as $\mathbf{r}_c = -l/k_\perp \mathbf{u}'(\varphi)$, is a ring.

3. Experiment

To produce the shaping nondiffracting structured caustic beams, we construct an experimental system based on the stationary phase principle, as shown in Fig. 3. An He–Ne laser is extended and successively incident on the phase plate and the axicon. The phase plates shown in Figs. 1(a2)–1(d2) are machined using a laser direct-writing system. Moreover, in the optical path, two polarizers are added to improve the quality of the generated caustic beams. Notably, in our experimental system, the light field did not pass through the narrow annular pupils given in Ref. [31]. The light field modulated by the phase element is incident on the surface of the axicon. Thus, the utilization of the effective light source area is increased, and the utilization rate of the light energy is improved. After the axicon, the modulated beam is diffracted; hence, the desired caustic beams are generated. In general, transverse caustics are recorded at 80 cm after the axicon, as shown in Figs. 4 and 5. We separately record the experimental diffraction patterns for astroid, deltoid, cardioid, and pentagram caustics. The experimental results are highly consistent with the simulation results of caustic beams. These results indicate the feasibility of our scheme in generating nondiffracting caustic beams with any required high-intensity curve in the transverse profile of the light field.

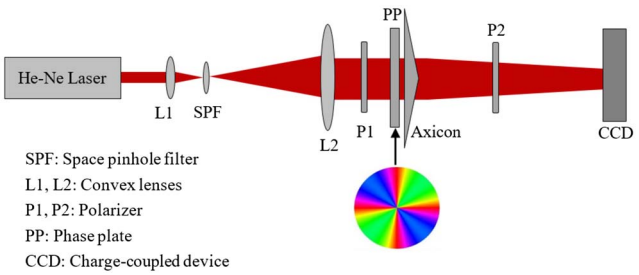

Fig. 3. Experimental system of generating caustic beams.

In accordance with the optical parameters of the experimental system, the fact that the maximum nondiffraction propagating distance of the generated caustic is $z_{max} = 1083$ mm can be readily known. To verify the transmission characteristics of the generated astroid caustic within the range of $z < z_{max}$, we simulate the astroid caustic in different propagation distances and record the intensity distribution in the corresponding propagation distances after the axicon, as shown in Fig. 6. This figure illustrates that the main structure of the beams is steady, and the optical intensity distribution of the astroid caustic is shape-preserved during propagation, although the optical intensity of the beams slowly increases during propagation. Hence the generated caustic beams on the basis of the stationary phase principle can be regarded as nondiffracting beams, similar to nondiffracting Bessel beams generated using an axicon. The optical lattice is an artificial light structure that is widely used in various branches of science, such as in trapping ultracold atomic

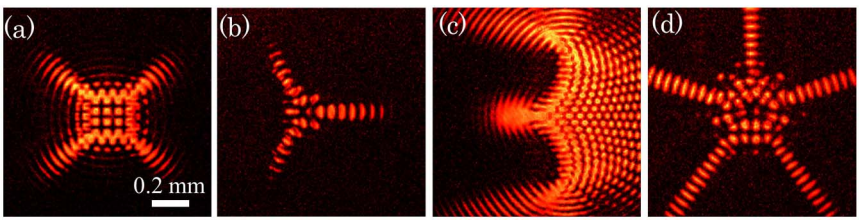

Fig. 4. Experimental recorded graphs of nondiffracting caustic beams with the same parameters as that in Fig. 1.

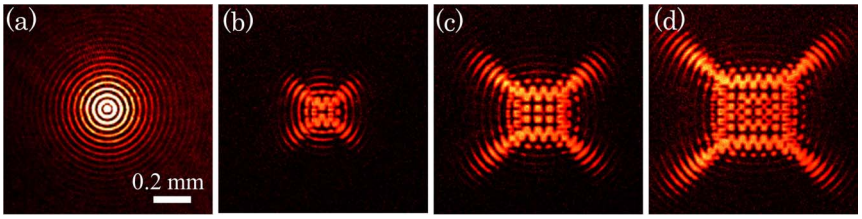

Fig. 5. Experimental recorded graphs of astroid caustic beams with the same parameters as that in Fig. 2.

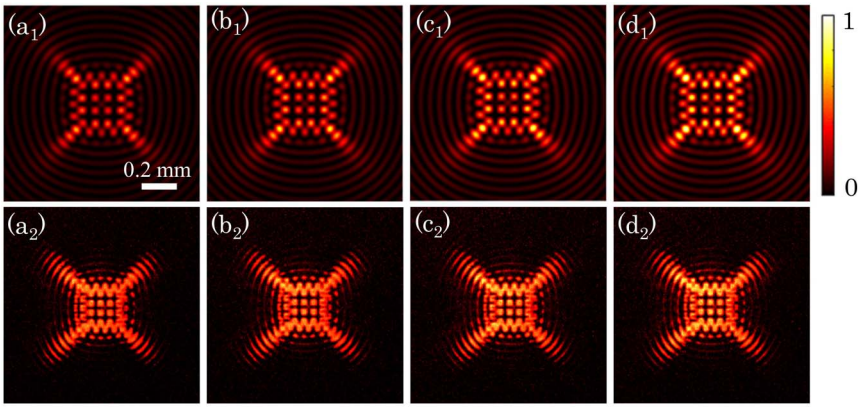

Fig. 6. Astroid caustic beams at different propagation distances after the axicon. (a1)–(d1) Simulation intensity graphs; (a2)–(d2) experimental recorded intensity graphs. Propagation distances: (a1), (a2) $z = 50$ cm; (b1), (b2) $z = 60$ cm; (c1), (c2) $z = 70$ cm; (d1), (d2) $z = 80$ cm.

gases[39–41] and in quantum computation[42]. In Ref. [43], Rechtsman reported that 2D caustic light with lattice features and well-defined curve boundaries could fabricate novel topological photonic structures. Apparently, our introduced high-efficiency method for generating nondiffracting structured caustic beams is expected to be applied conveniently to some potential landscapes.

4. Conclusion

We provide the first and novel generating mechanism of nondiffracting caustic beams on the basis of the stationary phase principle. Here, we obtain the analytic expression of astroid caustic beams for the first time on the basis of the stationary phase principle. Then, astroid, deltoid, cardioid, and pentagram caustic beams are experimentally observed. The experimental results agree well with the numerical simulation, demonstrating that the stationary phase principle is an effective method for producing the desired shaping nondiffracting structured caustic beams. Compared with the classical method of generating caustic beams using the Fourier transform method, the stationary phase method considerably improves the utilization efficiency of light energy. Apparently, we demonstrate a powerful approach for the high-efficiency generation of various desired nondiffracting caustic beams with customizable intensity profiles.

Acknowledgement

This work was supported by the National Natural Science Foundation of China (No. 11974314).

References

1. R. Thom, "Stabilite structurelle et morphogenese," Poetics **3**, 7 (1974).
2. V. I. Arnold, *Catastrophe Theory* (Springer, 1984).
3. T. Poston, *Stewart I Catastrophe Theory and Its Applications* (Dover Publications, 2014).
4. Y. A. Kravtsov and Y. I. Orlov, *Caustics, Catastrophes and Wave Fields* (Springer, 1999).
5. J. F. Nye, "Natural focusing and fine structure of light caustics and wave dislocations," Am. J. Phys. **68**, 776 (2000).
6. M. V. Berry and C. Upstil, "IV catastrophe optics: morphologies of caustics and their diffraction patterns," Prog. Optics. **18**, 257 (1980).
7. A. Zannotti, *Caustic Light in Nonlinear Photonic Media* (Springer, 2020).
8. A. Zannotti, F. Diebel, M. Boguslawski, and C. Denz, "Optical catastrophes of the swallowtail and butterfly beams," New. J. Phys. **19**, 053004 (2017).
9. H. Whitney, "On singularities of mappings of Euclidean spaces. I. Mappings of the plane into the plane," Ann. Math. **62**, 374 (1955).
10. V. I. Arnold, "Singularities of smooth mappings," Russ. Math. Surv. **23**, 1 (1968).
11. M. V. Berry, J. F. Nye, and F. J. Wright, "The elliptic umbilic diffraction catastrophe," Philos. Trans. Royal Soc. A **291**, 453 (1979).
12. J. Nye, "Dislocation lines in the hyperbolic umbilic diffraction catastrophe," Proc. Royal Soc. A. **462**, 2299 (2006).
13. G. A. Siviloglou and D. N. Christodoulides, "Accelerating finite energy Airy beams," Opt Lett. **32**, 979 (2007).
14. G. A. Siviloglou, J. Broky, A. Dogariu, and D. N. Christodoulides, "Observation of accelerating Airy beams," Phys. Rev. Lett. **99**, 213901 (2007).

15. Y. Wang, "Pearcey beam tuning and caustic evolution," J. Opt. Soc. Am. A **38**, 1726 (2021).
16. E. Greenfield, M. Segev, W. Walasik, and O. Raz, "Accelerating light beams along arbitrary convex trajectories," Phys. Rev. Lett. **106**, 213902 (2011).
17. Y. Lan, Y. Fu, and Y. Qian, "Generation of spirally accelerating optical beams," Opt. Lett. **44**, 1968 (2019).
18. I. Epstein and A. Arie, "Arbitrary bending plasmonic light waves," Phys. Rev. Lett. **112**, 023903 (2014).
19. A. Minovich, A. E. Klein, N. Janunts, T. Pertsch, D. N. Neshev, and Y. S. Kivshar, "Generation and near-field imaging of Airy surface plasmons," Phys. Rev. Lett. **107**, 116802 (2011).
20. L. Li, T. Li, S. M. Wang, C. Zhang, and S. N. Zhu, "Plasmonic Airy beam generated by in-plane diffraction," Phys. Rev. Lett. **107**, 126804 (2011).
21. J. Lin, J. Dellinger, P. Genevet, B. Cluzel, F. D. Fornel, and F. Capasso, "Cosine-Gauss plasmon beam: a localized long-range nondiffracting surface wave," Phys. Rev. Lett. **109**, 093904 (2012).
22. L. Li, T. Li, S. M. Wang, and S. N. Zhu, "Collimated plasmon beam: nondiffracting versus linearly focused," Phys. Rev. Lett. **110**, 046807 (2013).
23. I. J. Macias, C. R. Parrao, O. D. J. C. Rosas, E. E. Ramos, S. A. J. Reyes, P. O. Vidals, G. S. Ortigoza, and C. T. S. Sanchez, "Wavefronts and caustics associated with Mathieu beams," J. Opt. Soc. A. **35**, 267 (2018).
24. A. B. Chong, B. E. Portillo, A. C. Benavides, and S. L. Aguayo, "Asymmetric Mathieu beams," Chin. Opt. Lett. **16**, 122601 (2018).
25. Y. Hu, D. Bongiovanni, Z. Chen, and R. Morandotti, "Periodic self-accelerating beams by combined phase and amplitude modulation in the Fourier space," Opt. Lett. **38**, 3387 (2013).
26. P. Vaveliuk, A. Lencina, J. A. Rodrigo, and O. M. Matos, "Caustics, catastrophes, and symmetries in curved beams," Phys. Rev. A. **92**, 033850 (2015).
27. Y. H. Wen, Y. J. Chen, Y. F. Zhang, H. Chen, and S. Y. Yu, "Tailoring accelerating beams in phase space," Phys. Rev. A. **95**, 023825 (2017).
28. L. Froehly, F. Courvoisier, A. Mathis, M. Jacquot, M. Furfaro, R. Giust, P. A. Lacourt, and J. M. Dudley, "Arbitrary accelerating micron-scale caustic beams in two and three dimensions," Opt. Express **19**, 16455 (2011).
29. P. Vaveliuk, A. Lencina, and O. M. Matos, "Caustic beams from unusual powers of the spectral phase," Opt. Lett. **42**, 4008 (2017).
30. J. F. Nye, "Evolution of the hyperbolic umbilic diffraction pattern from Airy rings," J. Opt. A. Pure. Appl. Opt. **8**, 304 (2006).
31. A. Zannotti, C. Denz, M. A. Alonso, and M. R. Dennis, "Shaping caustics into propagation-invariant light," Nat. Commun. **11**, 3597 (2020).
32. J. H. McLeod, "The axicon: a new type of optical element," J. Opt. Soc. Am. **44**, 592 (1954).
33. G. B. Arfken, H. J. Weber, and F. Harris, *Mathematical Methods for Physicists* (Academic, 2000).
34. J. J. Stamnes, *Waves in Focal Regions: Propagation, Diffraction and Focusing of Light, Sound and Water Waves* (Taylor & Francis Group, 1986).
35. A. A. Kovalev, V. V. Kotlyar, and A. P. Porfirev, "Shifted nondiffractive Bessel beams," Phys. Rev. A. **91**, 053840 (2015).
36. S. Tu, Q. Lei, Y. Cai, and Q. Zhao, "Generation of Lommel beams through highly scattering media," Chinese Opt. Lett. **20**, 092501 (2022).
37. Z. Pi, Y. Hu, Z. Chen, and J. Xu, "Large-scale sharply bending paraxial beams," APL Photonics **4**, 056101 (2019).
38. I. G. Palchikova, "Diffraction-free beams and their caustics," Opt. Lasers Eng. **29**, 333 (1998).
39. M. Aidelsburger, M. Atala, S. Nascimbene, S. Trotzky, Y. A. Chen, and I. Bloch, "Experimental realization of strong effective magnetic fields in an optical lattice," Phys. Rev. Lett. **107**, 255301 (2011).
40. L. M. Duan, E. Demler, and M. D. Lukin, "Controlling spin exchange interactions of ultracold atoms in optical lattices," Phys. Rev. Lett. **91**, 090402 (2003).
41. I. Bloch, "Ultracold quantum gases in optical lattices," Nat. Phys. **1**, 23 (2005).
42. G. K. Brennen, C. M. Caves, P. S. Jessen, and I. H. Deutsch, "Quantum logic gates in optical lattices," Phys. Rev. Lett. **82**, 1060 (1999).
43. M. C. Rechtsman, J. M. Zeuner, Y. Plotnik, Y. Lumer, D. Podolsky, F. Dreisow, S. Nolte, M. Segev, and A. Szameit, "Photonic Floquet topological insulators," Nature **496**, 196 (2013).